ICSV 21
13-17 July, 2014, Beijing/China

The 21st International Congress on Sound and Vibration

13-17 July, 2014, Beijing/China

ASSESSMENT OF TRACK-GROUND COUPLED VIBRATION INDUCED BY HIGH-SPEED TRAINS

Jou-Yi Shih, David Thompson, Antonis Zervos

ISVR, University of Southampton, Southampton, SO17 1BJ, UK

e-mail: js10e12@soton.ac.uk

As high-speed trains operate in more and more countries and their maximum speed increases, the vibration induced by the train has become an important issue. The dynamic coupling between the vehicle, track and ground has to be assessed for its effects on safety, stability and maintenance costs. A particular issue, especially for soft soils, is the critical speed at which the train reaches the wave speed in the ground leading to large deflections of the track and ground. The aim of this paper is to develop a three-dimensional time-domain approach that describes how the moving dynamic loads of a high-speed train are distributed through the track components. This model should allow the critical speed to be determined and the vibration of the whole system to be analysed. To represent the complex vehicle/track/ground system a finite element approach is used based on the ABAQUS software. Rather than using a user-defined subroutine to apply the moving loads, the multi-body vehicle model and track/ground system are coupled as deformable bodies using a contact model that allows for large scale motion of the vehicle relative to the track.

1. Introduction

With the development of high-speed trains, which operate in more and more countries, and as their maximum speed increases, the vibration induced by the train has become an important issue. The dynamic coupling between the vehicle, track and ground has to be assessed for its effects on safety, stability and maintenance costs. A particular issue, especially for soft soils, is the critical speed at which the train reaches the wave speed in the ground. This can lead to large deflections of the track and ground and may lead to damage of the railway system.

Such critical speed effects will happen when the speed of a high-speed train exceeds the speed of waves in the ground and embankment. Dieterman and Metrikine used a model of a beam on a half-space to indicate that another critical speed, slightly smaller than the Rayleigh wave speed, exists and can also produce severe amplifications of the beam displacement.[1] However, the vehicle, tracks, and ground systems are not independent; each system is coupled to the others. Therefore, the assessment of these effects requires coupled vehicle-track-ground numerical simulations for better understanding of the dynamic behaviour of each component.

An analytical vehicle-track-ground interaction model, including wheel-rail interaction, was introduced by Sheng et al.[2] Moreover, they included dynamic loads as well as the quasi-static moving loads, representing the vehicle by a 10 dof multi-body model[3]. In addition, Sheng et al. developed a 2.5D Finite Element/Boundary Element (FE/BE) formulation in the frequency domain[1].

Karlström et al. combined an analytical ground model with a numerical vehicle/track model operating in the time domain and including a multi-body vehicle model[4]. A novel technique, called

the moving finite element method, was developed by Lane et al. to model the 3D multi-body vehicle/track/ground interaction for better efficiency and smaller model size[5]. In this, the soil material is moved relative to the FE mesh after a certain number of time steps, so that the vehicle does not need to move relative to the mesh.

A fully three-dimensional analysis of high-speed train-track-soil-structure dynamic interaction in the time domain was developed by Galvín using a coupled FE/BE method[6]. Kourossis et al. use a special technique to calculate the vehicle/track and track/ground analyses separately by assuming a much larger stiffness of the soil, compared to the stiffness of the ballast[7]. Infinite elements were used in ABAQUS for the boundaries of the ground model and were combined with a finite element model of the soil and a 5 degree-of-freedom multi-body vehicle to model 3D vehicle/track/soil dynamic interaction. Comparisons of numerical results in the time domain with measurements showed good agreement[7]. Recently, Connolly et al.[8] used a similar method but introduced a moving load subroutine, defined by FORTRAN code, into the ABAQUS model. Vehicle/track/ground interaction was simulated in the time domain and has been verified using experimental data collected from the high speed line between Paris and Brussels. Kacimi et al.[9] determined the dynamic response from the 3D finite element coupled train-track model by using the same approach but using a half rectangular ground model and the influence of the soil material damping was investigated.

A method of modelling the vehicle-track-ground interaction is presented here using the commercial FE software ABAQUS. The model operates in the time domain and it is intended that it will eventually account for vertical, lateral and longitudinal loading; it will include the dynamic behaviour of the vehicle (using a multi-body approach) and the wheel/rail contact as well as the track and the ground. A specific contact model is used in ABAQUS to allow the moving load or vehicle, instead of using a user-defined subroutine, as this reduces the cost of the simulation. To demonstrate the approach, example results are presented for a simple vehicle moving across a beam. Then the full track-ground system is introduced in which the ground is modelled using finite elements, with infinite elements used for the boundary. Finally, an assessment of the critical speed is given using a simple model of an ICE3 high-speed train for a track on a soft half-space ground.

2. Modelling moving vehicle problems

2.1 Simulation procedure

The response of a finite element system to a moving load can be readily calculated by specifying the nodal forces corresponding to the moving load as a function of time. However, for a moving vehicle problem, the loads depend on the dynamic response of the vehicle as well as the track system. Therefore, a user-defined subroutine is often used to combine a vehicle multi-body model with the FE model of the track. This requires more time to complete the simulation due to the interaction between the two different programs. To overcome this, an alternative approach has been adopted, using the large (finite) sliding contact model in ABAQUS[10].

Following the same procedure as Saleeb et al.[11], the approach has been tested on a simple moving vehicle-bridge interaction problem, simulated without the need for coupling with an external subroutine. In summary, this method requires an initial static analysis and then the execution of an implicit dynamic analysis based on the results from the previous step. This approach has been implemented here in ABAQUS. The node-to-surface contact feature is used to simulate the sliding motion on a frictionless surface and the default contact property ‘hard contact’ without contact damping is used. A constant moving speed is implemented by defining the displacement of the moving object along the direction of travel at each time step.

2.2 Simply supported beam with moving sprung mass

To demonstrate the method, a sprung mass moving along a simply supported beam is considered, as used by Saleeb et al.[11], as shown in Fig. 1. The dynamic response is compared with the numerical results obtained by Yang and Yau[12]. The material parameters adopted for the beam are: Young's modulus E=2.87 GPa, Poisson's ratio v=0.2, second moment of area I=2.94 m^4, mass density ρ=2303 kg/m^{-1}. The suspension stiffness is 1595 kN/m, damping is 0 Ns/m, and the mass is 5750 kg. The vehicle speed is 27.78 m/s and the length of the bridge, L, is 25m. The displacement of the beam and the sprung mass are shown in Fig. 2. These show good agreement with the results from Yang and Yau[12]. The difference in the beam response introduced by the dynamics of the sprung mass can also be seen by comparison with the results for a moving load in Fig. 2(a).

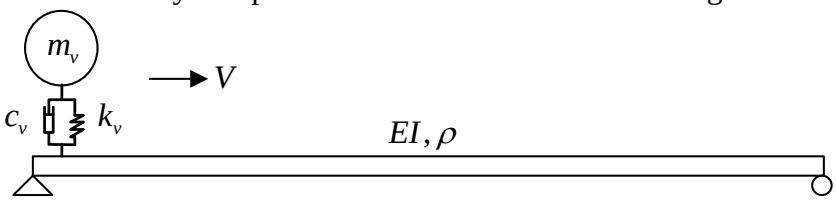

Figure 1. Moving oscillator with a simply support beam

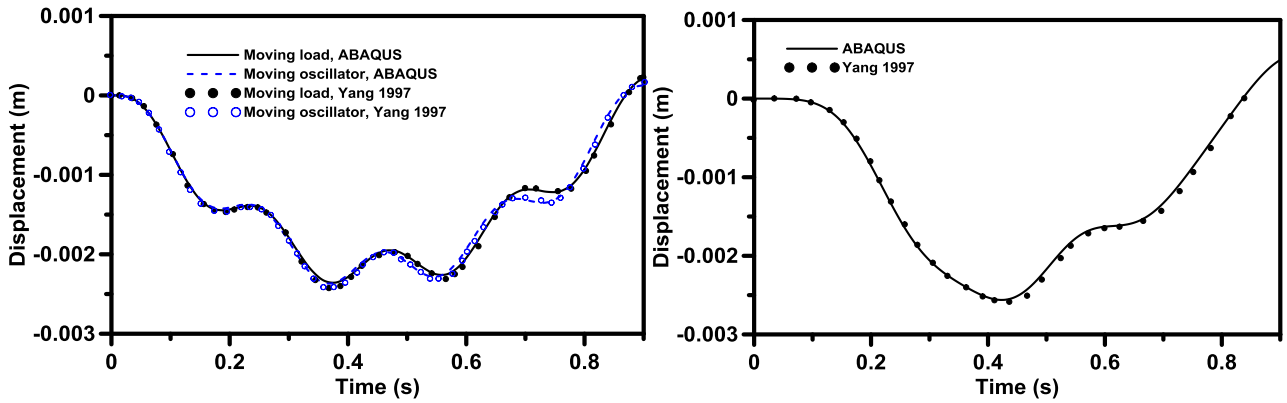

Figure 2. Vertical displacement of the beam and moving sprung mass; (a) midpoint displacement of the beam; (b) displacement of the sprung mass

3. Modelling of vehicle-track-ground interaction

Having established the method of coupling the moving vehicle to the FE model, a three-dimensional model of the vehicle-track-ground system is developed using ABAQUS. Modelling of the track system is described in section 3.1 and the ground system in section 3.2. A symmetry plane is introduced through the centreline of the track to decrease the cost of the simulation, as indicated in Fig. 3(a). Therefore, displacements in this plane in the z (transverse) direction are constrained.

3.1 Track model (rail, railpad, sleeper and ballast)

The track consists of UIC60 rail supported on railpads, sleepers and a layer of ballast, as shown in Fig. 3(b). The railpads and sleepers are represented by equivalent continuous models. Eight-node brick elements (C3D8) are used to model the rail, railpads and sleepers. The rail is represented by an equivalent rectangular cross-section with the same mass and bending stiffness as the UIC60 section. Homogeneous material is used for the whole track model except the sleepers. Although the equivalent sleeper layer is continuous along the axial direction, it should have no bending stiffness in this direction. Therefore, it is modelled using a transversely isotropic material. Four-

node tetrahedral elements (C3D4) are used for the ballast for compatibility with the ground surface. Tie constraints are used between the railpad and sleeper and between the sleeper and ballast as this provides a simple way to bond surfaces together by setting master-slave formulations. This constraint prevents the slave nodes from separating or sliding relative to the master surface; therefore, there are no relative displacements between the two surfaces. The parameters of the track are shown in Table 1.

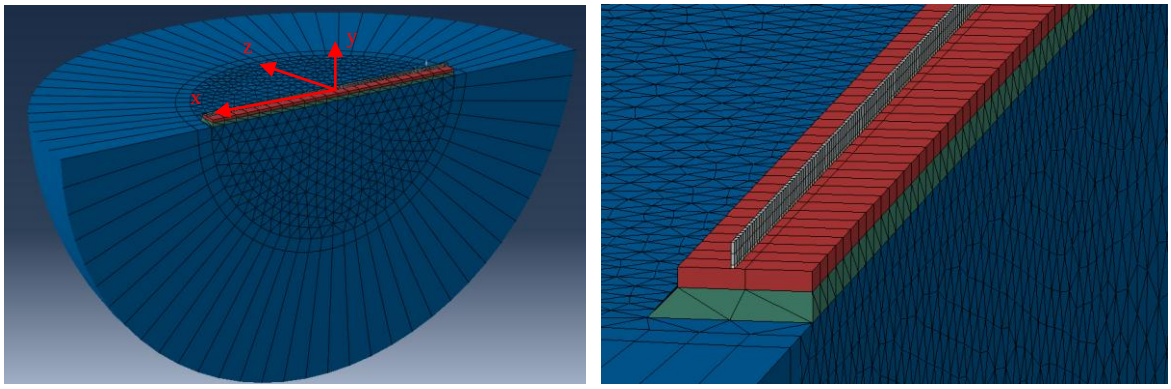

(a) (b)

Figure 3. Three-dimensional track/ground model; (a) whole model; (b) detail of the track model

Table 1. Track properties

Parameter	Value	Unit
Rail distance from symmetry plane	0.75	m
Rail mass	60	kg/m
Rail bending stiffness	6.4×10^{6}	Nm^2
Rail Poisson's ratio	0.3	
Rail pad stiffness	5×10^{8}	N/m^2
Half sleeper length	1.3	m
Sleeper height	0.2	m
Sleeper equivalent density	1042	kg/m^3
Sleeper equivalent Young's modulus (E_y, E_z)	1.25×10^{10}	N/m^2
E_x	0	N/m^2
Sleeper Poisson's ratio	0.15	
Ballast depth (below sleeper)	0.3	m
Half ballast width at top	1.3	m
Half ballast width at bottom	1.6	m
Ballast Young's modulus	4.8×10^{8}	N/m^2
Ballast density	2000	kg/m^3
Ballast Poisson's ratio	1/3	

3.2 Ground model (finite and infinite elements)

The ground is assumed to be a homogeneous half-space, with the properties listed in Table 2. It is represented as a quarter sphere of finite elements surrounded by infinite elements, as shown schematically in Fig. 4. The radius is chosen as 20 m. As for the track, use is made of symmetry in the *x-y* plane. Eight-node brick elements (C3D8) and four-node tetrahedral element (C3D4) are used for the ground model and eight-node linear, one-way infinite elements (CIN3D8) are introduced on the boundary in order to avoid wave reflections from the boundary.

A spherical model is used due to the importance of the position of the nodes in the infinite elements with respect to the origin. Infinite elements only give perfect absorption for waves that impinge perpendicularly to the boundary. Therefore, the spherical shape is preferred to a cuboid shape as it ensures that the vectors of the circular propagating wavefronts due to a point loading are almost normal to the boundary, as shown in Fig. 4. In addition, a Python code has been developed to construct the infinite elements combined with the finite element ground model automatically.

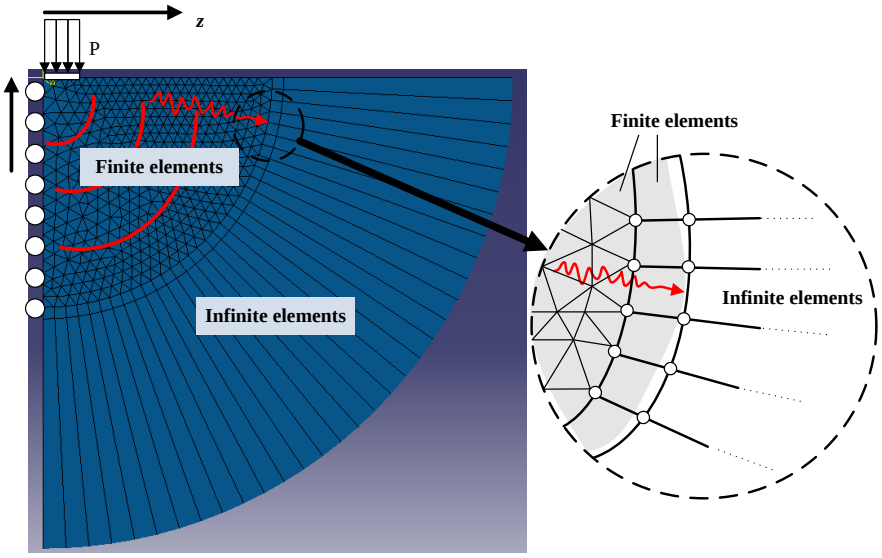

Figure 4. Schematic view of model geometry

Table 2. Ground properties

Young's Modulus, E	19.2 MN/m^2
Poisson's ratio, ν	0.33
Rayleigh damping	$\alpha = 0,\ \beta = 0.000159$
Mass density, ρ	2000 kg/m^3
P-wave speed, c_p	120 m/s
S-wave speed, c_s	60 m/s

Due to the inclusion of infinite elements, two types of analysis, Static General and Dynamic Implicit, are used. The solution of the static analysis is based on the work of Zienkiewicz et al.[13] and the infinite element for the dynamic analysis was developed by Lysmer and Kuhlemeyer[14]. The incident waves are absorbed by many dashpots which are oriented normal and tangential with respect to the boundary. The elements are designed to absorb plane waves in three orthogonal directions. Hence, the distributed equivalent dampers on the boundary are chosen to satisfy

$$\begin{cases} \sigma_{xx} = -\rho c_p \dot{u}_x \\ \sigma_{xy} = -\rho c_s \dot{u}_y \\ \sigma_{xz} = -\rho c_s \dot{u}_z \end{cases}. \tag{1}$$

where σ_{xx} etc are stresses, $\dot{u}_x$ etc are velocities, ρ is the material density and c_p, c_s are the wave speeds of the P-wave (longitudinal wave) and the S-wave (transverse wave) respectively.

3.3 Correction for rigid-body motion

As the ground model is unconstrained statically, a moving load causes the whole ground to rotate and translate, as shown in Fig. 5. It is not possible to constrain the ground in a way that is consistent with the infinite elements. Therefore, the rigid body motion is removed in a post-processing step.

The rigid body displacements, in terms of vertical, horizontal, and rotational displacements, are obtained from the mean values of the displacements over the boundary. The corrected displacements, as a function of time, at position (x,y,z) are obtained as follows:

$$\begin{cases} u' = u - \bar{u} - \dfrac{4R \cdot \overline{wx}}{\pi R^2} + y \dfrac{2 \cdot \overline{wx}}{R^2} \\ v' = v - \bar{v} - x \dfrac{2 \cdot \overline{wx}}{R^2} \end{cases} . \tag{2}$$

where v, u, are the vertical and horizontal displacements and $\bar{v}$, $\bar{u}$ are the average vertical and horizontal rigid body displacements obtained from the boundary at a given time step, as shown in Fig. 5. $\overline{wx}$ is the average horizontal displacement multiplied by the original position x. Finally, new horizontal and vertical displacements, u' and v', can be derived.

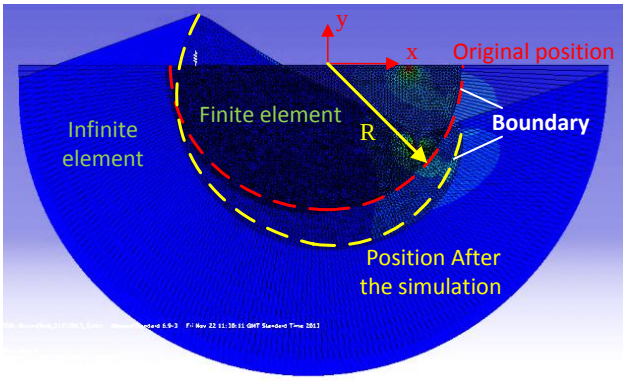

Figure 5. Rigid body motion occuring due to motion of the load

4. Numerical example

In this section, dynamic results of a vehicle/track/ground interaction are discussed and compared with the results without the vehicle model. The ground and track properties were introduced in section 3.1 and 3.2. The train parameters are based on an ICE3 high-speed train. Models based on a moving load and a moving sprung mass model are used to assess the critical speed. The axle load is 55757.6 N, the stiffness of the primary suspension is $.8.05\times10^5$ N/m, and mass of the sprung mass is 4924.75 kg.

Dynamic responses are shown in Fig. 6 in the form of the displacement at the midpoint of the model (x=0) as a function of load position. Results are shown for different moving load speeds. A higher maximum amplitude can be found when the vehicle speed is close to the shear wave speed, 60 m/s. However, the maximum displacement reduces again when the vehicle speed becomes higher. In addition, it can be seen that the response becomes asymmetric as the speed increases further. The maximum downward displacement occurs after the load has passed, while the positive (upward) displacement in front of the load is found to increase and reach a maximum when the vehicle speed is 83.33m/s, as shown in Fig. 6. This positive displacement may cause problems which should be taken into account in the design as well.

The ratio of the maximum downwards displacement to the static response is shown in Fig. 7(a) as a function of vehicle speed. This shows clearly that the response reaches a maximum when the load speed is around the shear wave speed of the ground. When the train speed is 60 m/s, the amplitude of the dynamic responses will be around 1.6 times higher than the static results for the ground and 1.4 times higher for the rail (note that the static response of the ground is smaller than that of the rail). The load position corresponding to the maximum displacement is shown in Fig. 7(b). This position shifts to around 2~2.5m when the speed is higher than 100 m/s.

Finally, the moving vehicle results are compared with the moving load result in Fig. 7(a). Although the vehicle model is simplified to a single mass-spring system, slight differences can be seen between the results.

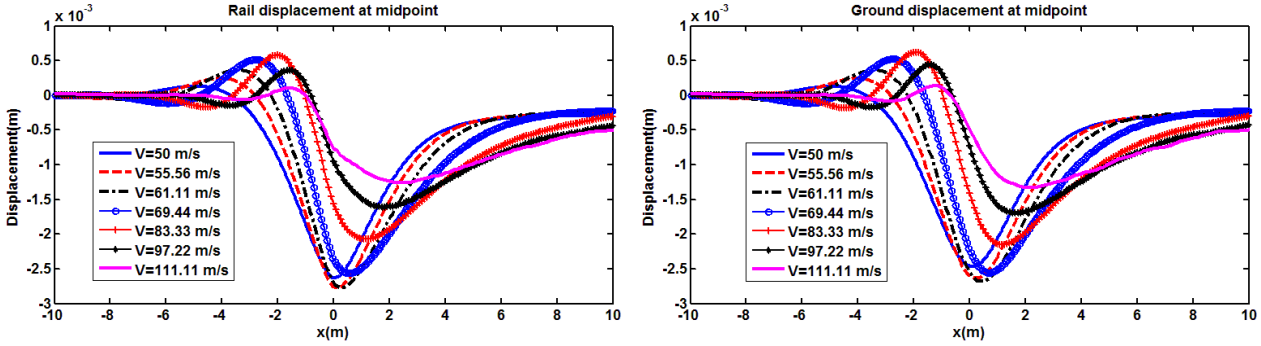

Figure 6. Midpoint displacement (at x=0) as a function of load position; (a) rail displacement; (b) ground displacement

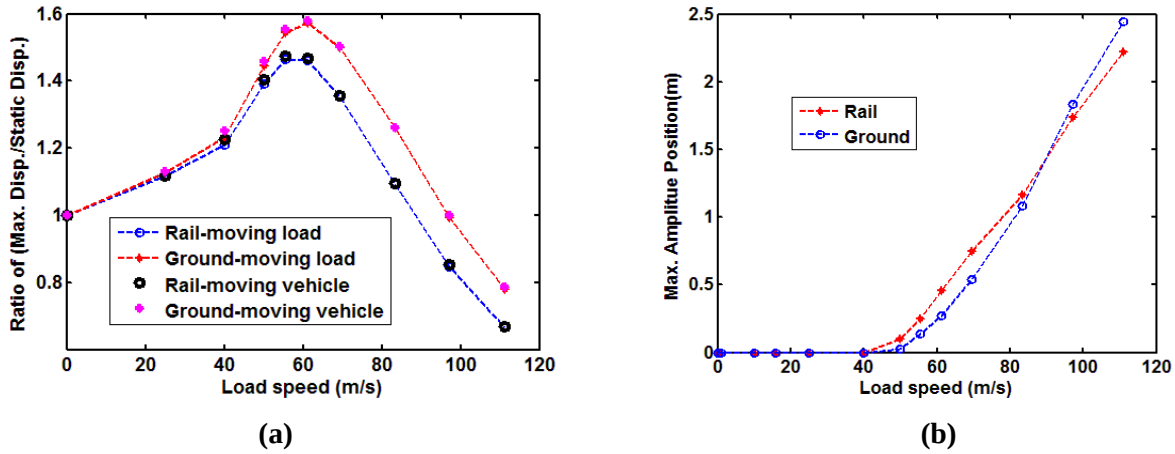

Figure 7. Maximum response and location of the maximum response along the x-axis on the rail and the ground. (a) ratio of maximum displacement to static displacement; (b) position of maximum displacement

5. Conclusions

A three-dimensional time-domain model of a coupled vehicle, track and ground has been developed in the FE software ABAQUS. The ground is represented using finite and infinite elements. A new analysis approach has been adopted for modelling the moving vehicle without the need for a user-defined subroutine. Rigid-body motion of the ground occurs due to the unconstrained boundary but this has been solved by removing the dynamic rigid-body response as a function of time in a post-processing step. The results allow the critical speed to be determined and the vibration of the

whole system to be analysed. More complete train models can be considered using this approach as well as the effect of ground nonlinearity; these will be considered in the future.

Acknowledgements

The work described has been supported by the EPSRC under the programme grant EP/H044949/1, 'Railway Track for the 21st Century'.

REFERENCES

1 Dieterman, H. A., Metrikine, A., The equivalent stiffness of a half-space interacting with a beam. Critical velocities of a moving load along the beam, *European Journal of Mechanics A/Solids*, **15**, 67-90, (1996).

2 Sheng, X., Jones, C. J. C., Thompson, D. J., A theoretical model for ground vibration from trains generated by vertical track irregularities, *Journal of Sound and Vibration*, **272**(3)-(5), 937-965, (2004).

3 Sheng, X., Jones, C. J. C., Thompson, D. J., A comparison of a theoretical model for quasi-statically and dynamically induced environmental vibration from trains with measurements, *Journal of Sound and Vibration*, **267**, 621-635, (2003).

4 Sheng, X., Jones, C. J., Thompson, D. J., Modelling ground vibration from railways using wavenumber finite-and boundary-element methods, Proc. R. Soc. A, **461**, 2043-2027, (2005). Karlström, A., Nielsen, J., Boström, A., Train/track-soil numerical-analytical interaction model in the time domain, *Chalmers Applied Mechanics*, Research Report 2006:8, Gothenburg 2006 (also listed as VB8:6)

5 Lane, H., Kettil, P., Wiberg, N., Moving finite elements and dynamic vehicle interaction, *European Journal of Mechanics A/Solids*, **27**, 515-531, (2008).

6 Galvín, P., Romero,A., Domínguez, J., Fully three-dimensional analysis of high-speed train-track-soil-structure dynamic interaction, *Journal of Sound and Vibration*, **329**, 5147-5163, (2010).

7 Kourossis, G., Verlinden, O., Conti, C., Ground propagation of vibrations from railway vehicles using finite/infinite-element model of the soil, *Proceedings of the Institution of Mechanical Engineers*, Part F: Journal of Rail and Rapid Transit, **223**(4), 405-413, (2009).

8 Connolly, D., Giannopoulos, A., Forde, M. C., Numerical modelling of ground borne vibrations from high speed rail lines on embankments, *Soil Dynamics and Earthquake Engineering*, **46**, 13-19, (2013).

9 Kacimi, A. E., Woodward, P. K., Laghrouche, O., Medero, G., Time domain 3D finite element modelling of train-induced vibration at high speed, *Computers and Structures*, **118**, 66-73, (2013).

10 ABAQUS 6.11 Theory Manual.

11 Saleeb, Atef F., Kumar, Abhimanyu, Automated finite element analysis of complex dynamics of primary system traversed by oscillatory subsystem, *International Journal for Computational Methods in Engineering Science and Mechanics*, **12**, 187-202, (2011).

12 Yang, Y. B., Yau, J. D., Vehicle-bridge interaction element for dynamic analysis, *Journal of Structural Engineering*, **123**, 1512-1518, (1997).

13 Zienkiewicz, O. C., Emson,C., Bettess, P., A novel boundary infinite element, *International Journal for Numerical Methods in Engineering*, **19**(3), 393-404, (1983).

14 Lysmer, J., Kuhlemeyer, R., Finite dynamic model for infinite media, *Journal of Engineering Mechanics*, **95**(EM4), 859-877, (1969).